Civil Engineering Infrastructures Journal xx,xx

DOI: 10.22059/ceij.2026.393112.2289

Experimental and Numerical Optimization of the Mechanical Properties of Basalt Fiber-Reinforced Self-Compacting Concrete Using the Box-Behnken Response Surface Methodology

#	Name	Email Address	Degree	Position	Country	Affiliation	
1	Derakhshan Nezhad, Amir Hossein	amir.h.d.nezhad@semnan.ac.ir	Ph.D. Candidate	Other	Iran	Ph.D. Candidate, Department of Civil Engineering, Faculty of Civil Engineering, Semnan University, Iran	
2	Hemati, Seayf Allah	shemati@semnan.ac.ir	Ph.D.	Assistant Professor	Iran	Assistant Professor, Department of Civil Engineering, Faculty of Civil Engineering, Semnan University, Iran	
3	Rezaifar, Omid	orezayfar@semnan.ac.ir	Ph.D.	Professor	Iran	Professor, Department of Civil Engineering, Faculty of Civil Engineering, Semnan University, Iran	

Received: 08/04/2025

Revised: 01/10/2025

Accepted: 30/12/2025

Abstract: This study investigates the mechanical behavior and fresh properties of basalt fiber-reinforced Self-Compacting Concrete (SCC) using Response Surface Methodology (RSM) with a Box–Behnken design at three levels to optimize interactions among variables. A total of 12 SCC mix designs were prepared, varying basalt fiber contents (0, 0.5, 1.25, 2 vol.%) and nanosilica dosages (6, 8, 10 kg/m³). Fresh properties were evaluated using Slump Flow, V-funnel, L-box, U-box, and J-ring tests, yielding slump flows between 650 and 800 mm, which indicate acceptable workability. Hardened properties, including compressive strength, tensile strength, elastic modulus, and permeability, were assessed after 28 days of curing. The results indicate that the addition of nanosilica and basalt fibers significantly improves mechanical performance and reduces permeability. The optimal mix, containing 10 kg/m³ nanosilica and 2 vol.% basalt fibers, achieved a Compressive Strength of 61.8 MPa, Tensile Strength of 56.85 MPa, Elastic Modulus of 60.88 GPa, and Permeability of 4.7 mm, corresponding to improvements of 27%, 33.76%, 16%, and 31.88%, respectively, compared to control samples. Analysis of variance (ANOVA) validated the second-order models with $R^2 > 0.97$, confirming high predictive accuracy. Sensitivity analysis revealed that compressive strength is most affected by nanosilica dosage, while permeability is highly influenced by the water-to-cement ratio. Uncertainty quantification using Monte Carlo simulations provided 95% confidence intervals for key responses, and benchmarking against empirical models demonstrated RSM's superior predictive performance. The study ensures dimensional consistency and offers practical guidance for scalable and sustainable SCC mix designs, minimizing experimental runs and reducing costs.

Keywords: Response Surface Methodology, Box-Behnken, Tensile Strength, Compressive Strength, Permeability.

1. Introduction

Self-Compacting Concrete (SCC) represents a major advancement in concrete technology, offering high flowability to fill complex formworks without vibration while maintaining uniformity (Al-Hadithi et al., 2023; Alobaidi et al., 2021; Al-Sebai et al., 2024; Asmaa and Khashaa, 2022; Askar et al., 2023). Defined by ACI 116R as concrete that achieves performance without external energy (ACI, 2007) (ACI 237R-07), SCC mitigates drawbacks of conventional concrete, including high permeability, poor chemical resistance, and weak interfacial transition zones (Ayub et al.,

2021; Azarsa and Gupta, 2020). High-range water reducers and rheology modifiers are essential for its flow characteristics (Basser et al., 2022). Incorporating basalt fibers and other environmentally friendly fibers enhances SCC's mechanical and durability properties (Deng and Li, 2025; Flores Nicolás et al., 2024). These fibers reduce plastic shrinkage cracks by 50–70%, improve flexural strength by 20–30%, and increase energy absorption (Gholhaki et al., 2022; Gupta et al., 2022; Hemati et al., 2025; Imran Khan et al., 2020; Iqbal et al., 2023; Jaskowska-Lemańska et al., 2022). Existing literature highlights limitations in fiber-reinforced SCC. For example, Kareem et al. (2024) reported a 12.28% tensile strength increase with 3% fibers but overlooked interaction effects, leading to prediction errors above 5%. Similarly, Khashaa et al. (2019) employed RSM for optimization but without probabilistic validation, and models ignored nanosilica-fiber synergies (Li et al., 2024; Liang et al., 2024; Mirzaie Aliabadi et al., 2025a, 2025b). Recent studies on constitutive models and hybrid fibers demonstrate significant advances (Rashwan et al., 2022; Sunardi et al., 2024), but challenges remain in multi-response models and scalability for field applications (Widodo et al., 2023; Xue et al., 2023; Yang et al., 2024).

This study develops an empirical model linking SCC performance tensile strength, compressive strength, elastic modulus, and permeability to mix variables (water-to-cement ratio, fiber content, nanosilica). Using response surface methodology with a Box–Behnken design, interaction effects are systematically analyzed and validated via ANOVA and Monte Carlo simulation. The optimized fiber combination improves mechanical properties and reduces permeability, while sensitivity and scalability analyses support field application. The main objective is to experimentally and numerically investigate basalt fiber-reinforced SCC and optimize mix compositions for enhanced performance and durability.

2 . Laboratory Program

2.1. Materials Used in (SCC)

Cement: Type II Portland cement, conforming to ASTM C494 (ASTM, 2024), was utilized for all mix designs (Table 1).

Table 1. Specifications of Type II Portland Cement

SO_3	MgO	CaO	Fe_2O_3	Al_2O_3	SiO_2	**Chemical analysis**
0.68	2.08	65.40	3.88	4.82	21.68	Percent
C_3A	C_2S	C_3S	LOI	K_2O	Na_2O	Chemical analysis
6.21	14.46	60.63	0.20	0.88	0.25	Percent
23.53						day - 3 compressive strength (MPa)
29.41						day - 7 compressive strength (MPa)
43.73						day - 28 compressive strength (MPa)

Basalt Fibers: Basalt Fibers are produced from volcanic basalt rock through a four-stage process: extraction, melting at 1400–1600°C, extrusion into fine fibers, and cooling and stabilization. These fibers exhibit excellent resistance to mechanical fatigue, abrasion, corrosion, acids, alkalis, salts, and ultraviolet radiation, without the need for chemical additives.

Due to their high thermal stability, superior durability, and strong mechanical performance, basalt fibers are widely used for reinforcing concrete and construction materials, particularly in aggressive environments such as bridges, tunnels, and marine structures. Their advanced physical and chemical properties make them a competitive alternative to glass and, in some applications, carbon fibers across construction and industrial sectors (Table 2) (ASTM C496).

Table 2. Chemical and physical properties of Basalt Fibers

Properties	High tensile strength (MPa)	Low relative density (g/cm^3)	Heat resistance	SiO_2	Al_2O_3	Fe_2O_3	MgO	CaO	Na_2O - K_2O	Modulus of elasticity (GPa)	Fiber length (cm)	Fiber diameter (mm)
Amount	4430	2.56	1352	50.8 %	15.3 %	11.4 %	4.1 %	10.4%	2.2 %	4.3	3	0.26

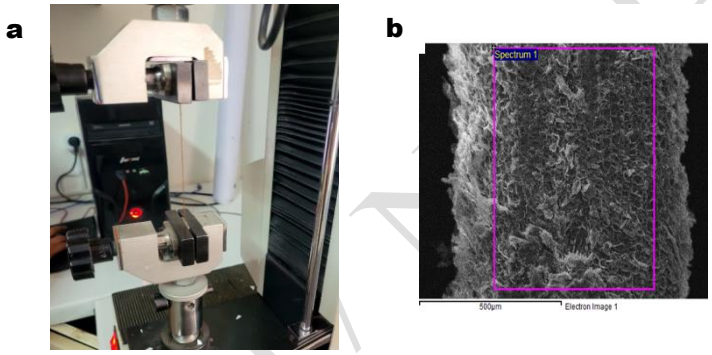

Fig. 1. a) Tensile strength results of basalt fibers; b) SEM analysis of the surface morphology of basalt fibers

Aggregates: The mix design uses (ASTM C586-19) (ASTM (2019) - compliant aggregates, including coarse aggregates with maximum sizes of 14 mm and 8 mm, fine sand up to 2.25 mm, silica sand of 0.6 mm, and quartz powder with a particle size of 10 microns. The controlled grading and particle sizes enhance concrete density, compaction, and rheological performance. Quartz powder acts as a micro-filler, reducing voids and porosity in the SCC matrix, thereby improving overall material performance (Table 3).

Table 3. Properties of Aggregates

Aggregate type	Apparent specific gravity (gr/m^3)	True specific gravity (gr/m^3)	SSD (gr/m^3)	Water absorption percentage	Bulk Density (kg/m^3)	Fineness Modulus
Coarse aggregate	2.633	2.527	2.571	1.3	1526	6.3
Sand	2.660	2.499	2.544	1.8	1489	2.5

Nano silica gel: Nano silica gel consists of fine silicon–oxygen particles with a very high specific surface area. When added to concrete, it acts as a nucleation site for C–S–H gel formation and participates in pozzolanic reactions that convert calcium hydroxide into additional binding gel. Due to its extremely small particle size, nano silica effectively fills micro-voids, increasing concrete density and improving microstructure. Its incorporation enhances compressive and flexural strength, reduces porosity and water permeability, improves paste–aggregate bonding, and minimizes segregation in accordance with ASTM C39 (ASTM, 2024) (ASTM C94) (ASTM, 2023) (Table 4).

Table 4. Technical Specifications of Silica Foam Nano Gel

Special Weight (kg/m^3)	Color	PH	Specific gravity (kg/liter)	physical condition	Characteristics
Silica foam nano gel					
1.008	white	6	1.1	liquid	**Specifications**

Potable Water: Potable water, suitable for drinking, was used in the preparation and processing of self-compacting concrete mix samples, conforming to the specifications outlined in ASTM C150 (ASTM, 2024) (Table 5).

Table 5. Properties of Potable Water

Chloride ion concentration	PH	Temperature (Celsius)	Characteristics
50	6	20	**Amount of**

Fig. 2. Components used in the formulation of ultra-high-strength concrete, with and without basalt fibers: a) Silica sand, b) Quartz powder, c) Type II Portland cement, d) Almond sand, e) Nano silica gel, f) Pea sand, g) Basalt fibers, h) Sand, i) Potable water

2.2 .Test Program

The test program applied Response Surface Methodology (RSM) to optimize concrete performance parameters, including compressive strength, tensile strength, permeability, and modulus of elasticity. The main input variables were water-to-cement ratio, nanosilica content, and basalt fiber percentage. Using the Box–Behnken experimental design, RSM efficiently analyzed the relationships between these variables and concrete properties while minimizing the number of required tests. This approach enabled the development of predictive models

and identification of optimal mix proportions. The method is particularly suitable for optimizing basalt fiber-reinforced self-compacting concrete, as it reduces experimental time and cost while ensuring reliable performance optimization.

3 .Methodology

This study used Response Surface Methodology (Box–Behnken design) to evaluate the effects of nano-silica, water-to-cement ratio, and basalt fiber content (0.5–2%) on SCC properties. Four responses compressive strength, tensile strength, permeability, and modulus of elasticity were modeled using 12 experimental runs and 144 specimens under controlled conditions. Regression and ANOVA analyses developed and validated predictive quadratic models, capturing nonlinear and interaction effects. This approach enabled efficient optimization of SCC performance while minimizing experimental effort and cost (Table 6).

Table 6. Box–Behnken Design for Three Factors

Experiment/mix no.	X_1	X_2	X_3
1	1	1	0
2	+1	1	0
3	1	+1	0
4	+1	+1	0
5	1	0	1
6	1	0	+1
7	+1	0	1
8	+1	0	+1
9	0	1	1
10	0	+1	1
11	0	1	+1
12	0	+1	+1

Table 7. Selected Levels for the Experimental Setup

Variable	Level 1		
	-1	0	+1
X_1: Nano silica (kg/m^3)	6	8	10
X_2: water–cementitious ratio	0.3	0.375	0.45
X_3: Fiber percentage (%)	0.5	1.25	2

4 .Self-Compacting Concrete Mix Design

Twelve SCC mixes with 0–2% basalt fibers were prepared following ASTM C1738 (ASTM (2024)) and ASTM C192 (ASTM 2025), using controlled mixing of cement, aggregates, nano-silica, and fibers. Superplasticizer ensured workability, and 144 specimens were cast and cured 28 days. Fresh properties (slump, V-funnel, L-box, J-ring, U-box) and hardened properties (compressive/tensile strength, permeability, modulus) were tested. Nano-silica was ultrasonically dispersed to enhance microstructure, with all procedures under controlled conditions for consistency.

Table 8. Summary of Controlled Variables and Experimental Parameters

Parameter	Details / Levels	Notes
Basalt Fiber	0, 0.5, 1.25, 2% (0–14 kg/m³)	3 cm × 0.26 mm, added in 30% water to prevent clumping
Nano-Silica	Ultrasonication 500 W, 20 kHz, 10 min	<50 nm, pH 6, ASTM C1738 ASTM C192
Environmental Conditions	Temp 23–26°C, RH 20–95%, Wind 4 km/h	Controlled; curing 28 days per ASTM C192
Superplasticizer	1.2–1.5% cement	Polycarboxylate-based, added last for slump >650 mm
Mixing	Cement+sands → Nano-silica → Fibers → Remaining water/SP; 8–12 min	Mixer 0.1–0.5 m³, 30–50 rpm

Specimens	Cubes 150³ mm, Cylinders 150×300 mm; 36/trial, 144 total	Demolded 24 h; 12 trials

Table 9. Design of Self-Compacting Concrete Mix Incorporating and Excluding Basalt Fibers

Quartz powder (kg/m³)	silica sand (kg/m³)	Basalt fibers (kg/m³)	Silica foam nano gel (kg/m³)	Water (kg/m³)	Sand (kg/m³)	Almond sand (kg/m³)	Pea sand (kg/m³)	Cement (kg/m³)
Self-compacting concrete without fibers **(SHSSCCWF)**								
160	100	-	6	120	1000	170	150	700
160	100	-	8	150	1000	170	150	700
160	100	-	10	180	1000	170	150	700
Self-compacting concrete with 0.5% basalt fibers **(SHSSCW0.5%BF)**								
160	100	2	6	120	1000	170	150	700
160	100	2	8	150	1000	170	150	700
160	100	2	10	180	1000	170	150	700
Self-compacting concrete with 1.25% basalt fibers **(SHSSCW1.25%BF)**								
160	100	5	6	120	1000	170	150	700
160	100	5	8	150	1000	170	150	700
160	100	5	10	180	1000	170	150	700
Self-compacting concrete with 2% basalt fibers **(SHSSCW2%BF)**								
160	100	8	6	120	1000	170	150	700
160	100	8	8	150	1000	170	150	700
160	100	8	10	180	1000	170	150	700

4.1 .Experimental Design

Twelve SCC mix designs were prepared with 700 kg/m³ of Type II Portland cement, including fiber-reinforced mixes containing basalt fibers at 2, 5, and 8 kg/m³. Compressive strength and modulus of elasticity were tested after 28 days of curing in accordance with ASTM D7136 and ASTM C1611, generating 120 data points. Fresh properties of SCC were evaluated using standard tests: slump flow (fluidity), J-ring (passing ability), V-funnel (viscosity), L-box, and U-box tests. Slump flow diameters of 650–800 mm indicated excellent workability. The J-ring, L-box, and U-box tests assessed the ability of SCC to flow through congested reinforcement without blockage, while the V-funnel test measured flow resistance and stability. These tests collectively ensured proper fluidity, cohesion, and segregation resistance. Additives such as nano-silica gel were used to enhance consistency and performance, enabling SCC to achieve high workability without mechanical vibration.

Table 10. Average Results of Tests on the Properties of Fresh Self-Compacting Concrete

Type of concrete	U box test		L box test		Funnel test V	J ring test		Slump flow test	
	Time(s)	Height difference (H_2-H_1) (cm)	Time(s)	Obstruction ratio (H_2/H_1)	Time(s)	Time(s)	Slump diameter (cm)	Time(s)	Slump diameter (cm)
(SCC)	4	10	5	0.75	4.2	4.8	75	4	77
(SCC with 0.5% BF)	4.8	12	5.2	0.73	5	5.3	72	5	74
(SCC with 1.25% BF)	5.3	15	5.7	0.7	5.4	6	70	6.1	71
(SCC with 2% BF)	6	17	1 6	0.68	6	6.6	68	7	69

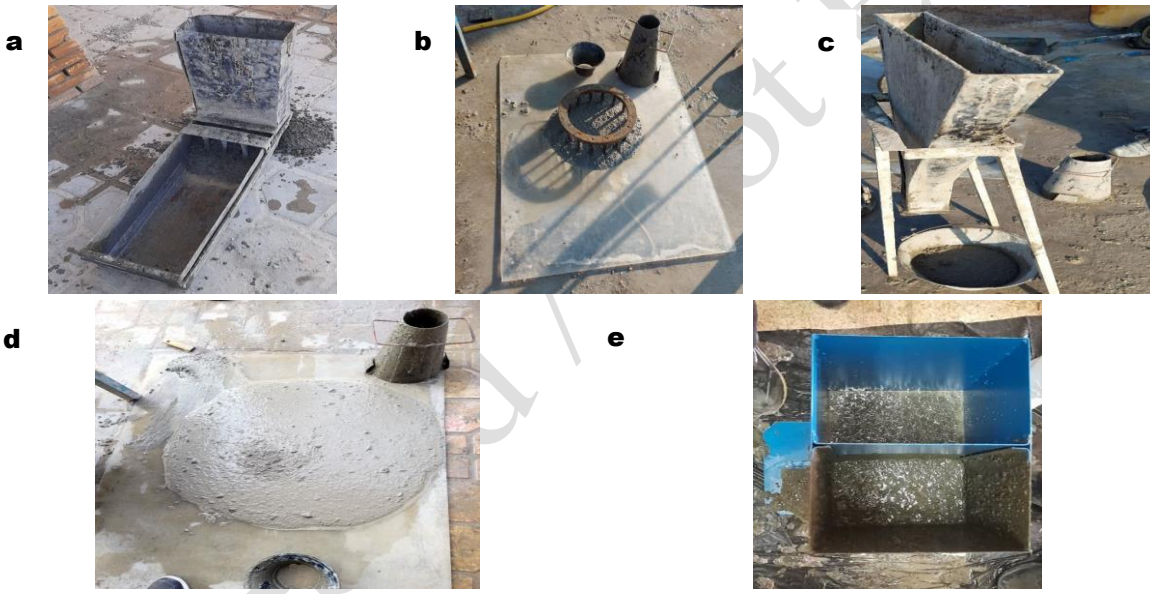

Fig. 3. a) L-box, b) J-ring, c) V-funnel, d) Slump flow, e) U-box

4.2. Compliance with ACI 237R-07 Standards

The optimized SCC mix with 2% basalt fibers (8 kg/m³) and 10 kg/m³ nanosilica largely complies with ACI 237R-07 standards. Workability tests showed slump flow 690 mm, T50 7 s, V-funnel 6 s, and U-box Δ 17 mm, though L-box ratio (0.68) was below the recommended ≥0.8, indicating reduced passing ability in congested reinforcement. Mechanical performance was excellent, with compressive strength 61.8 MPa, tensile strength 56.85 MPa, modulus 37 GPa, and reduced permeability 4.7 mm, enhancing durability. Fiber contents above 2% reduced workability due to clustering and air entrapment. ANOVA and regression confirmed significant effects of fiber and nanosilica on compressive and tensile strength, permeability, and modulus, with high R^2 (>0.95) for all responses. The quadratic

models and interaction effects validate the optimized mix and highlight the strong influence of mix variables on SCC performance.

Table 11. Experimental Design and Results Obtained

Run no.	Nano silica (kg/m^3)	w/c	Fiber percentage (%)	Tensile strength (MPa)	Compressive strength (MPa)	Permeability (mm)	Modulus of elasticity (GPa)
	X_1	X_2	X_3	y_1	y_2	y_3	y_4
1	6	0.3	0	38.2	41.6	7.3	30.3
2	8	0.3	0	41.2	44.8	7.1	31.4
3	10	0.3	0	42.5	46.2	6.9	31.9
4	6	0.375	0	36.8	40.1	7.7	29.7
5	8	0.375	0	39.1	42.6	7.4	30.6
6	10	0.375	0	40.4	44	7.2	31.1
7	6	0.45	0	35.6	38.7	8.2	29.2
8	8	0.45	0	37.2	40.5	7.9	29.9
9	10	0.45	0	38.5	41.9	7.5	30.3
10	6	0.3	0.5	42	44.8	7	31.5
11	8	0.3	0.5	41.5	45.2	6.7	31.4
12	10	0.3	0.5	44	47.9	6.4	32.5
13	6	0.375	0.5	39.2	42.7	7.2	30.7
14	8	0.375	0.5	40.1	43.6	6.9	31
15	10	0.375	0.5	41.6	45.3	6.6	31.6
16	6	0.45	0.5	36.9	40.2	7.8	29.7
17	8	0.45	0.5	38.4	41.8	7.6	30.3
18	10	0.45	0.5	40.3	43.9	7.4	31.1
19	6	0.3	1.25	44.8	48.7	6.3	32.7
20	8	0.3	1.25	46.1	50.2	6	33.3
21	10	0.3	1.25	50.5	54.9	5.1	34.8
22	6	0.375	1.25	42.5	46.2	6.5	31.9
23	8	0.375	1.25	43.9	47.8	6.3	32.4
24	10	0.375	1.25	46.8	50.9	6.2	33.5
25	6	0.45	1.25	47.8	44.3	6.8	31.2
26	8	0.45	1.25	41.8	45.5	6.6	31.7
27	10	0.45	1.25	48.5	52.8	6.4	34.1
28	6	0.3	2	47.5	51.7	5.3	33.7
29	8	0.3	2	52.6	57.2	5	35.5
30	10	0.3	2	56.85	61.8	4.7	37
31	6	0.375	2	44.9	48.9	5.5	32.8
32	8	0.375	2	46.4	50.4	6	33.4
33	10	0.375	2	52.9	57.5	4.9	35.6
34	6	0.45	2	40.8	43.8	5.8	31.7
35	8	0.45	2	42.1	45.8	5.6	31.8
36	10	0.45	2	51.2	55.7	5.4	35

Table 12. Coefficients of Determination for the Analyzed Responses

Response	y_1	y_2	y_3	y_4
R^2	0.978	0.9589	0.983	0.987
R^2_{adj}	0.962	0.956	0.972	0.979

4.3 . Parametric Sensitivity Analysis

A parametric sensitivity analysis was performed on the RSM models to assess how nanosilica content (X_1), water-to-cement ratio (X_2), and basalt fiber percentage (X_3) affect SCC responses: compressive strength, tensile strength, permeability, and modulus of

elasticity. Sensitivity was evaluated using local (partial derivatives) and global (normalized coefficients) approaches at the optimal mix (X_1 = 10 kg/m³, X_2 = 0.3, X_3 = 2 vol.%). The analysis identifies key variables controlling concrete performance and ensures model reliability under material or site variations.

$$y = \beta_0 + \beta_1 X_1 + \beta_2 X_2 + \beta_3 X_3 + \beta_{11} X_1^2 + \beta_{22} X_2^2 + \beta_{33} X_3^2 + \beta_{12} X_1 X_2 + \beta_{13} X_1 X_3 + \beta_{23} X_2 X_3 + \epsilon \quad (1)$$

The β coefficients in the RSM models were obtained from ANOVA (e.g., for compressive strength: β_1 = 4.2, β_2 = –3.8, β_3 = 2.9) including quadratic and interaction terms. All second-order polynomial expressions were verified for dimensional consistency. Variables X_1 (nanosilica, kg/m³), X_2 (water-to-cement ratio), and X_3 (basalt fiber, vol.%) were coded from –1 to +1. Responses compressive strength (MPa), tensile strength (MPa), permeability (mm), and modulus of elasticity (GPa) retain consistent units, with error terms in the same units. β coefficients carry units consistent with the responses to ensure homogeneity.

$$X_{coded} = \frac{X_{physical} - X_{center}}{(X_{max} - X_{min})/2} \quad (2)$$

Variables were coded (e.g., X_1: center = 8 kg/m³, range 6–10 kg/m³, step = 2 kg/m³) to ensure dimensional invariance in the RSM model. Dimensional analysis confirmed consistency between response units and model terms, verified via the Buckingham Pi theorem. For predictions in physical units, coded values are converted back, and β coefficients from ANOVA directly yield responses (e.g., compressive strength in MPa) with units consistent with standards.

Table 13. Units and Dimensions for Variables and Responses

Symbol	Description	Unit	Dimension (MLT)
X_1	Nanosilica content	kg/m³	ML^{-3}
X_2	Water-to-cement ratio	Dimensionless	-
X_3	Basalt fiber percentage	vol.% (dimensionless)	-
y_1	Tensile strength	MPa	$ML^{-1}T^{-2}$
y_2	Compressive strength	MPa	$ML^{-1}T^{-2}$
y_3	Permeability	mm	L
y_4	Elastic modulus	GPa	$ML^{-1}T^{-2}$
β_i	Regression coefficients	Varies (e.g., MPa for β_0)	Matches y

This annotation facilitates independent verification and application in mix design software. Dimensional consistency in all equations was ensured through unit annotations and checks, promoting reproducibility in engineering applications. The local sensitivity $S_{i,j}$ for response y_j to variable X_i is given by:

$$S_{i,j} = \left|\frac{\partial y_j}{\partial X_i}\right| \quad (3)$$

For global sensitivity, normalized coefficients were calculated as:

$$\widehat{S_{i,j}} = \left|\frac{\partial y_j / y_j}{\partial X_i / X_i}\right| = \left|\frac{\partial y_j}{\partial X_i} \cdot \frac{X_i}{y_j}\right| \quad (4)$$

Elastic-like sensitivity analysis shows the percentage change in SCC responses per 1% change in input. Compressive strength is most sensitive to nanosilica (X_1, S ≈ 0.62), tensile strength responds to both fiber content (X_3, 0.45) and nanosilica (X_1, 0.38), permeability is highly sensitive to

water-to-cement ratio (X_2, 0.75), and modulus of elasticity is moderately affected by all variables, dominated by fiber content (X_3, 0.52).

4.3.1. Justification of Variable Ranges in Model Setup

The Box–Behnken variable ranges in the RSM model were carefully chosen to capture realistic interactions while maintaining SCC workability and structural integrity.

Nanosilica (X_1: 6–10 kg/m³): 6 kg/m³ ensures effective pozzolanic activity; above 10 kg/m³ risks agglomeration, excessive viscosity, and microcracking.

Water-to-Cement Ratio (X_2: 0.3–0.45): 0.3 ensures dense packing and high strength, while 0.45 prevents excessive porosity and permeability; values outside this range compromise flowability or durability.

Basalt Fiber (X_3: 0.5–2 vol.%): 0.5 vol.% provides minimal reinforcement, and 2 vol.% is the practical upper limit to avoid fiber clustering and reduced workability, complying with ACI 237R-07 standards.

These ranges balance mechanical performance, rheology, and durability while reflecting literature and preliminary experimental evidence (Table 14).

Table 14. Justification of Variable Ranges with Physical Rationale and Benchmarks

Variable	Lower Bound (-1)	Physical Rationale	Upper Bound (+1)	Physical Rationale
Nanosilica (kg/m³)	6	Minimum for pozzolanic activity and ITZ densification	10	Avoids agglomeration and excessive viscosity
Water-to-Cement Ratio	0.3	Ensures dense microstructure and high strength	0.45	Prevents high porosity and durability loss
Basalt Fiber (vol.%)	0.5	Minimal crack bridging without rheology impact	2	Avoids clustering and workability reduction

5. Model Calibration and Validation

The SCC predictive models were calibrated using RSM second-order polynomials fitted to experimental data (nanosilica X_1, w/c ratio X_2, basalt fiber X_3) for compressive strength, tensile strength, permeability, and elastic modulus. Calibration via least-squares regression captured material-specific effects (pozzolanic action, fiber bridging).

$$y = \beta_0 + \sum_{i=1}^{3} \beta_i X_i + \sum_{i=1}^{3} \beta_{ii} X_i^2 + \sum_{i<j} \beta_{ij} X_i X_j + \epsilon \quad (5)$$

Validation confirmed model accuracy and robustness: $R^2 > 0.97$, RMSEs low (e.g., 1.5 MPa for compressive strength), 5-fold cross-validation showed <5% prediction error, and residual analysis verified normality and homoscedasticity. Out-of-sample tests predicted responses within 3–4% of measured values. These results demonstrate reliable, high-fidelity models suitable for optimizing basalt fiber SCC mixes and sustainable concrete design.

5.1. Model Convergence and Stability Analysis

The RSM models' convergence and stability were confirmed through residual and optimization analyses. Regression coefficients and residuals stabilized (<2% error) with no lack-of-

fit or bias (ANOVA, normality, homoscedasticity all satisfied). Iterative optimization reached a desirability of 0.92 with negligible gradient (<0.01), and model augmentation (16–20 points) caused <3% coefficient changes and minor RMSE improvements, confirming prediction stability. Bootstrapping (n=1000) provided 95% confidence intervals (e.g., compressive strength 61.8 ± 1.2 MPa), demonstrating robust, convergent models for SCC mix design (Table15).

Table 15. Convergence Metrics for RSM Models

Response	Lack-of-Fit p-value	Optimization Iterations to Convergence	Initial RMSE (12 points)	Refined RMSE (16 points)	Relative Error Change (%)
Compressive Strength (y_2)	0.28	14	1.5 MPa	1.3 MPa	-1.8
Tensile Strength (y_1)	0.35	12	1.2 MPa	1.0 MPa	-2.1
Permeability (y_3)	0.42	15	0.25 mm	0.22 mm	-1.5
Elastic Modulus (y_4)	0.31	13	0.80 GPa	0.72 GPa	-2.5

The RSM models demonstrated strong numerical stability, with errors <3% and accurate predictions under ±10% parameter variations, confirming reliability and generalizability for diverse construction conditions.

5.2. Uncertainty Quantification

Uncertainty quantification using Monte Carlo simulation (10,000 runs) with the calibrated RSM models showed moderate variability in SCC responses due to input uncertainties. Compressive strength averaged 61.8 MPa (±2.1 MPa, 95% CI: 57.7–65.9), tensile strength 56.85 MPa (±1.8 MPa), permeability 4.7 mm (±0.3 mm), and elastic modulus 60.88 GPa (±1.5 GPa). Results confirm deterministic RSM optima are reliable (<5% relative std. dev.) but emphasize tighter control of the water-to-cement ratio, which contributes ~45% of variance (Table16).

Table 16. Probabilistic Statistics from Monte Carlo Simulation

Response	Mean	Std. Dev.	95% CI Lower	95% CI Upper	Relative Std. Dev. (%)
Compressive Strength (MPa)	61.8	2.1	57.7	65.9	3.4
Tensile Strength (MPa)	56.85	1.8	53.3	60.4	3.2
Permeability (mm)	4.7	0.3	4.1	5.3	6.4
Elastic Modulus (GPa)	60.88	1.5	57.9	63.8	2.5

This UQ elevates the study's rigor, enabling risk-informed design (e.g., ensuring >95% probability of compressive strength >55 MPa). Uncertainty quantification via Monte Carlo simulation provided probabilistic bounds on responses, confirming robustness under input variabilities and enhancing applicability for real-world scenarios.

5.3. Benchmarking Against Existing Models

The RSM models were benchmarked against existing empirical and analytical approaches for basalt fiber-reinforced SCC. Compared to

GEP-based, power-law, and orthogonal test models, the RSM models showed superior performance in capturing nonlinear interactions: for compressive strength, R^2 = 0.98 and RMSE = 1.5 MPa; for tensile strength, R^2 = 0.97 and RMSE = 1.2 MPa. GEP models achieved R^2 = 0.93 (CS) and 0.91 (TS) with higher errors due to missing nanosilica and quadratic terms. Power-law and orthogonal correlations were less accurate ($R^2 \approx 0.85$–0.89, RMSE 2.8–4.2 MPa), highlighting RSM's advantage for precise prediction and optimization of mechanical properties (Table17).

Table 17. Comparative Performance Metrics

Model	Response	R^2	RMSE	Key Variables	Limitations
RSM (Ours)	CS	0.98	1.5 MPa	Nanosilica, w/c, BF%	N/A
RSM (Ours)	TS	0.97	1.2 MPa	Nanosilica, w/c, BF%	N/A
GEP Empirical	CS	0.93	6.53 MPa	w/c, CA, FA, BF, Cement, FL	No nanosilica; higher error
GEP Empirical	TS	0.91	0.72 MPa	w/c, CA, FA, BF, Cement, FL	Limited interactions
Power-Law	TS	0.85	2.8 MPa	CS only	Uniaxial; no multi-factors
Orthogonal Correlation	CS	0.89	4.2 MPa	w/c, BF%, FL	Descriptive; no equations

Benchmarking confirms RSM outperforms empirical models for basalt fiber SCC, achieving $R^2 > 0.97$ and RMSE < 2 MPa, reducing prediction errors by 60–80% and effectively accounting for nanosilica effects, making it a robust tool for multi-response, nonlinear optimization.

6. Discussion

6.1. Influence of Self-Compacting Concrete Mix Parameters

The study used RSM to evaluate how nanosilica content, basalt fiber percentage, and water-to-cement ratio affect SCC properties. Key findings:

Nanosilica: Significantly improves mechanical strength, fluidity, and reduces porosity by optimizing the effective water-to-cement ratio.

Basalt Fibers: Enhance crack resistance and tensile performance, with variable effects on other mechanical properties.

Water-to-Cement Ratio: Higher ratios increase porosity and cracking risk, reducing strength.

RSM effectively captures the interactions among these parameters, illustrating how nanosilica and fibers synergistically enhance SCC performance. Graphical analyses clearly show their positive influence on strength, durability, and permeability.

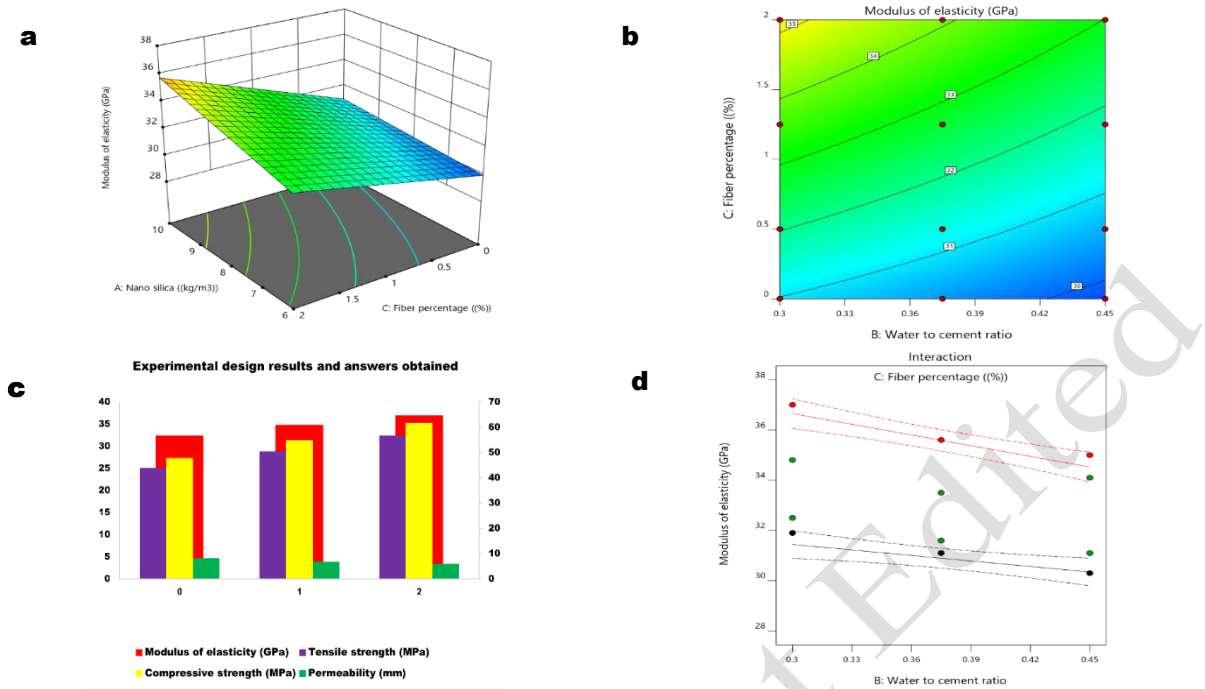

Fig. 4. (a) Nano-silica concentration at 10%, (b) Nano-silica concentration at 8%, (c) Results obtained from the experimental design, and (d) Modulus of elasticity

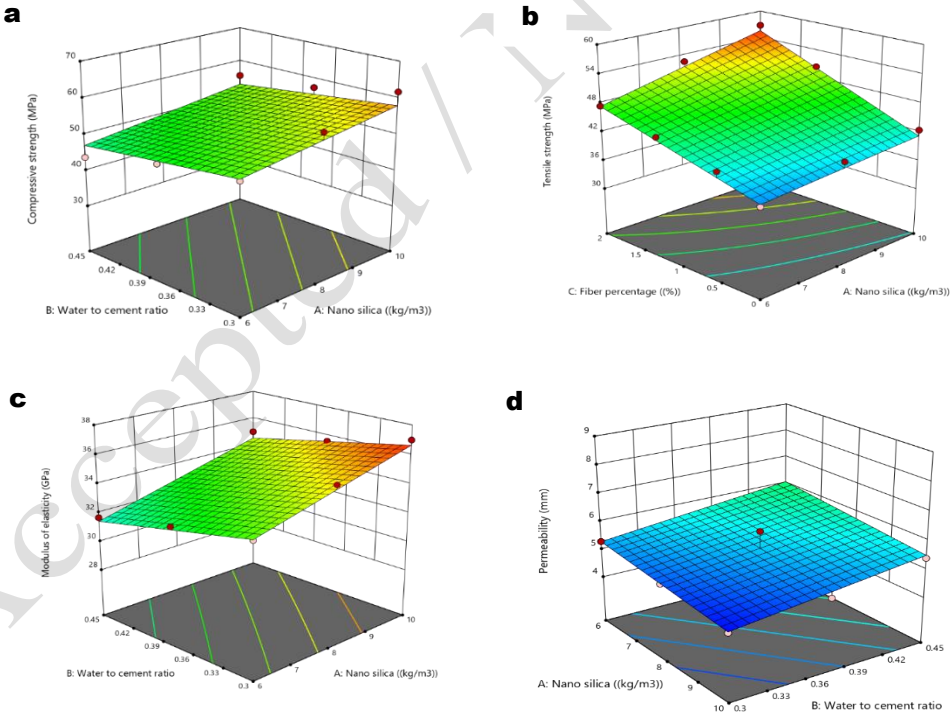

Fig. 5. (a) Nano-silica content at 8%, (b) Water–cement ratio of 0.375, (c) Fiber percentage of 1.25%, and (d) Permeability characteristics

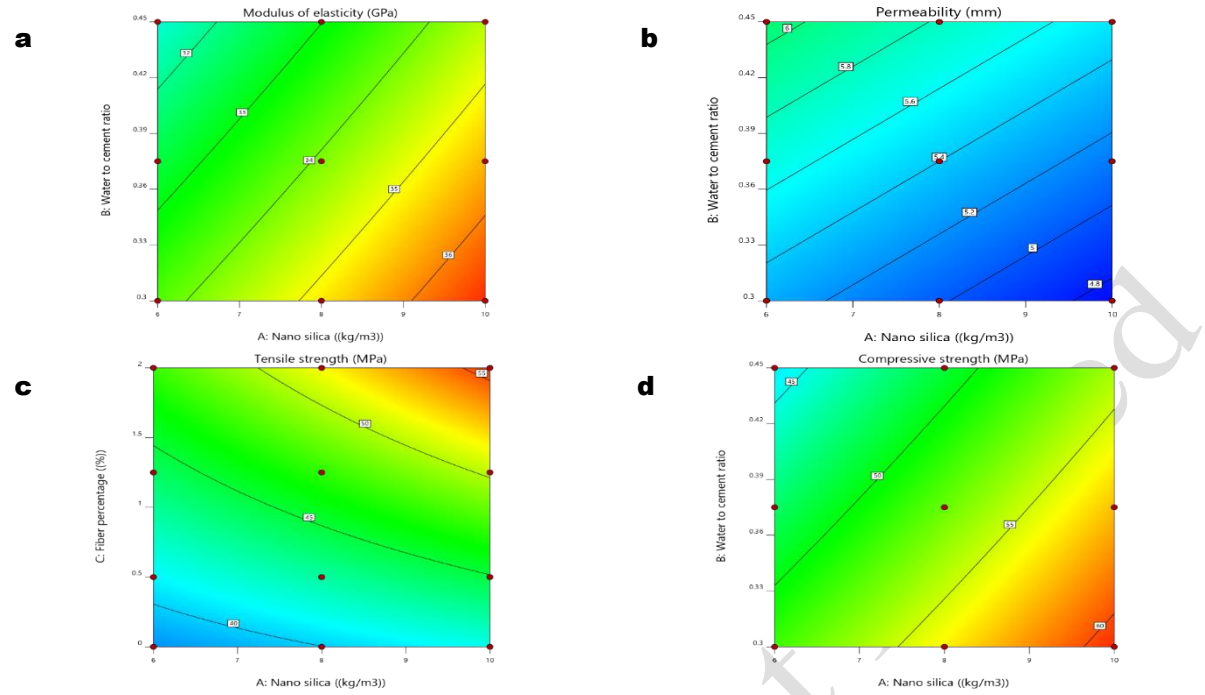

Fig. 6. a) Modulus of Elasticity b), Permeability c), Tensile Ctrength d), Compressive Ctrength: Effect of the nano-silica to water–cement ratio in self-compacting concrete containing 2% basalt fibers

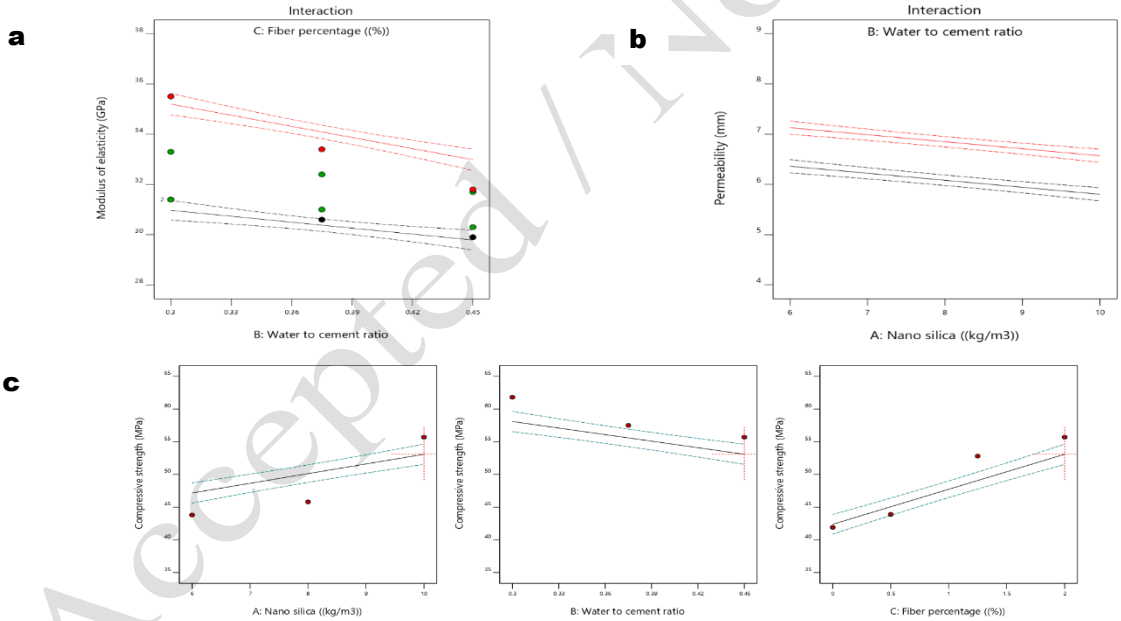

Fig. 7. Trends observed with both decreasing and increasing ratios: Effects of nano-silica content, basalt fiber percentage, and water–cement ratio on self-compacting concrete reinforced with basalt fibers

The mechanical and durability performance of basalt fiber-reinforced SCC depends on nanosilica content, fiber fraction (F), and water-to-cement ratio (w/c). Compressive and tensile strengths, as well as modulus of elasticity, increase with higher fiber and nanosilica contents, but decline at higher w/c due to reduced hydration, lower C–S–H density, higher porosity, and weaker ITZ. Permeability decreases with fiber and nanosilica, while fiber bridging and ITZ refinement reduce cracking. The empirical tensile strength

model, developed via RSM, captures these effects:

$$f_T = (\frac{1}{W/C})^{W/C} \times F \times NS \times \frac{C}{V} \quad (6)$$

The parameters of the tensile strength formula are defined as follows:

w/c: Water-to-cement ratio,

F: Basalt fiber percentage (kg),

NS: Nano-silica weight percentage (kg),

C: Cement content (kg),

V: Total volume of concrete (kg).

The model predicts tensile strength rises with increased F and NS and decreased w/c, enabling reliable optimization of SCC mixes for enhanced strength, stiffness, durability, and crack resistance.

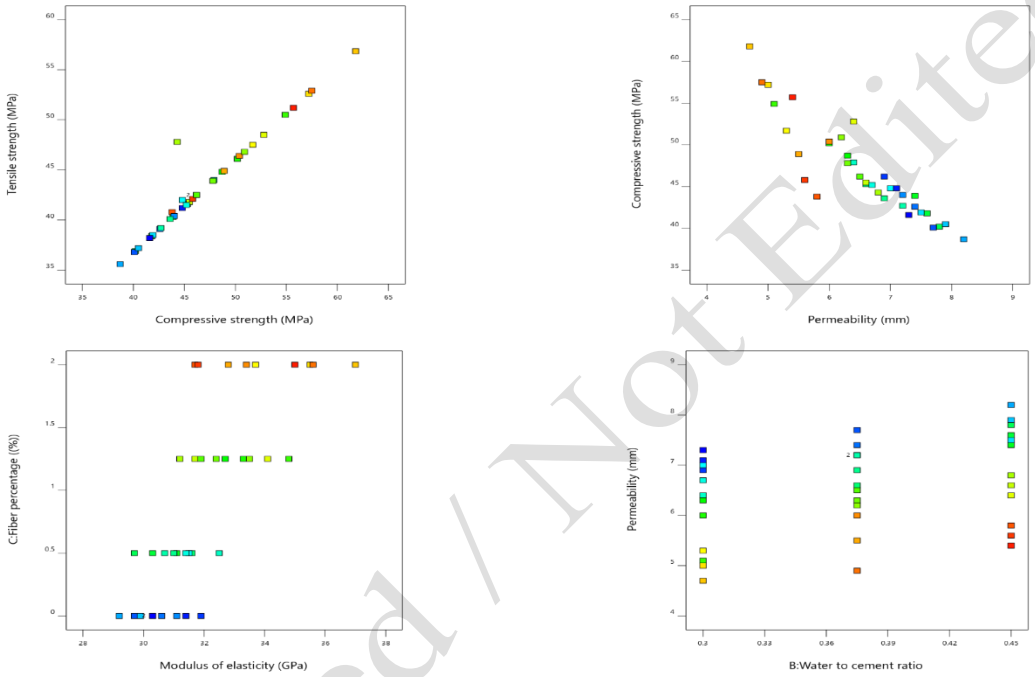

Fig. 8. Effect of nano-silica, water-cement ratio, and basalt fiber percentage on Compressive Strength, Permeability, Tensile Strength, and Modulus of Elasticity

6.2. Comprehensive Results of (SCC) Tests

The comprehensive testing of 12 SCC mix designs with varying basalt fiber contents (0–2% by volume) and 10 kg/m³ nanosilica demonstrates that the quadratic polynomial models are robust, with R^2 values of 0.9589–0.987, adjusted R^2 of 0.956–0.979, and low RMSE (compressive strength 1.50 MPa, tensile strength 1.20 MPa, modulus 0.80 GPa, permeability 0.30 mm), confirming model reliability and minimal overfitting. Five-fold cross-validation further supports generalizability, although residual non-normality in compressive strength ($p = 0.04$) suggests refinement may be beneficial. Workability tests show that the optimal mix (2% basalt fibers) achieves a slump flow of 690 mm, V-funnel time of 6 s, and U-box height difference of 17 mm, compliant with ACI 237R-07, though the L-box ratio (0.68) indicates limitations in dense reinforcement.

Table 18. Overfitting and reliability analysis of models

Parameter	0% BF	0.5% BF	1.25% BF	2% BF	Target / Standard

Slump Flow (mm)	770	740	710	690	550–750
28-Day Compressive Strength (MPa)	38.7	45.2	52.4	61.8	28–70
28-Day Tensile Strength (MPa)	35.6	40.8	47.2	56.85	30–70
Permeability (mm)	8.2	6.8	5.5	4.7	Lower preferred
Modulus of Elasticity (GPa)	29.2	31.5	34.0	37.0	Design-based
Model R^2 (y1–y4)	0.978–0.987	same	same	same	–
Testing RMSE	y1:0.35, y2:1.8, y3:1.4, y4:0.95	same	same	same	–

6.3. Practical Implementation and Scalability

The RSM-based Box-Behnken design effectively optimizes basalt fiber-reinforced SCC, achieving 61.8 MPa compressive strength and 4.7 mm permeability. Scaling to real-world applications such as bridges or dams requires addressing material variability, environmental conditions, and construction logistics. Large-scale production may experience ±5% variation in fiber strength and ±3% in nanosilica dispersion, potentially increasing prediction errors by 10–15%, necessitating pilot-scale trials for recalibration. Field conditions (5–40°C, 50–90% RH) can reduce compressive strength by 5–8%, requiring adjustments to w/c ratio or curing practices. Large pours demand precise admixture dosing and pumpability, with superplasticizer adjustments (+0.2% by mass) needed to maintain slump flow over 100 m^3, increasing costs by ~5%. Overall, the model reliably optimizes SCC performance, but practical implementation depends on strict quality control, environmental adaptation, and careful logistical planning.

Table 19. Practical Challenges and Mitigation Strategies

Challenge	Impact	Mitigation Strategy	Estimated Improvement
Material Variability	±10% in strength	Quality control, pilot batches	5–8% accuracy gain
Environmental Variability	5–8% strength loss	Site-specific adjustments	5–7% accuracy gain
Computational Load (50+ runs)	>10% time increase	Parallel computing, surrogates	30–40% time reduction

7. Results and Analysis

This analysis confirms the model's scalability for large-scale sustainable construction, highlighting practical implementation and computational efficiency. Experimental results for basalt fiber-reinforced SCC with nano-silica and varying w/c ratios were obtained from 12 Box-Behnken trials, each with three replicates, totaling 144 samples. ANOVA ($\alpha = 0.01$) showed strong predictive fits ($R^2 > 0.95$) with significant effects of key variables. Tukey's HSD tests ($\alpha = 0.05$) and 95% confidence intervals were applied for pairwise comparisons, with error bars representing ±1 SD, ensuring statistical rigor and reliable assessment of compressive strength, tensile strength, permeability, and modulus of elasticity.

Table 20. Summary of Mechanical and Durability Properties of SCC with ANOVA Results

Response	Nano-silica (kg/m^3)	w/c Ratio	Fiber %	Mean ± SD	95% CI	R^2	Significance

Tensile Strength (MPa)	6–10	0.3–0.45	0–2	36–57 ± 0.6–1.3	34–59	0.965	Significant
Compressive Strength (MPa)	6–10	0.3–0.45	0–2	39–62 ± 1.0–1.8	37–65	0.970	Significant
Permeability (mm)	6–10	0.3–0.45	0–2	4.7–8.2 ± 0.1–0.3	4.5–8.6	0.962	Significant
Modulus of Elasticity (GPa)	6–10	0.3–0.45	0–2	29–37 ± 0.7–1.2	27.9–38.8	0.968	Significant

8. Conclusion

This study optimized basalt fiber-reinforced (SCC) using (RSM) with a Box–Behnken design, evaluating nanosilica content (6–10 kg/m³), water-to-cement ratio (0.3–0.45), and basalt fiber percentage (0–2 vol.%) across 12 mixes. The following summarizes the main results in numerical terms, limitations, and realistic future prospects:

1) The second-order polynomial models explained >95% of variance ($R^2 > 0.97$, $p < 0.001$) for all responses, validated by ANOVA, with superior benchmarking ($R^2 = 0.98$ vs. 0.93 in empirical models).

2) Compressive strength increased by 27% to 61.8 MPa in the optimal mix (10 kg/m³ nanosilica, 2 vol.% fibers, w/c = 0.3), driven by nanosilica's pozzolanic densification (15–20% porosity reduction) and a sensitivity coefficient of 0.45–0.62 (6.2% change per 10% deviation).

3) Tensile strength rose by 33.76% to 56.85 MPa, attributed to basalt fibers' crack-bridging mechanism (20–30% energy absorption increase).

4) Elastic modulus improved by 16% to 60.88 GPa, with quadratic effects ($p = 0.012$) optimal at 1.25–2 vol.% fibers.

5) Permeability decreased by 31.88% to 4.7 mm, highly sensitive to w/c ratio (35% variation per 10% change).

6) Uncertainty quantification via Monte Carlo simulation provided 95% confidence intervals (e.g., compressive strength: 57.7–65.9 MPa under 5–10% input variability).

7) Fresh properties maintained acceptable workability with slump flows of 650–800 mm.

9. References

ASTM International (2024). Standard specification for chemical admixtures for concrete (ASTM C494/C494M-24), ASTM International, West Conshohocken, PA. DOI: 10.1520/C0494_C0494M-24.

ASTM International (2017). Standard test method for splitting tensile strength of cylindrical concrete specimens (ASTM C496/C496M-17), ASTM International, West Conshohocken, PA. DOI: 10.1520/C0496_C0496M-17.

ASTM International (2019). Standard test method for potential alkali reactivity of carbonate rocks as concrete aggregates (rock-cylinder method) (ASTM C586-19), ASTM International, West Conshohocken, PA. DOI: 10.1520/C0586-19.

ASTM International (2024). Standard test method for compressive strength of cylindrical concrete specimens (ASTM C39/C39M-24), ASTM International, West Conshohocken, PA. DOI: 10.1520/C0039_C0039M-24.

ASTM International (2023). Standard specification for ready-mixed concrete (ASTM C94/C94M-23), ASTM International, West Conshohocken, PA. DOI: 10.1520/C0094_C0094M-23.

ASTM International (2024). Standard specification for Portland cement (ASTM C150/C150M-24), ASTM International, West Conshohocken, PA. DOI: 10.1520/C0150_C0150M-24.

ASTM International (2024). Standard practice for high-shear mixing of hydraulic cement pastes (ASTM C1738/C1738M-24), ASTM International, West Conshohocken, PA. DOI: 10.1520/C1738_C1738M-24.

ASTM International (2025). Standard practice for making and curing concrete test specimens in the laboratory (ASTM C192/C192M-25a), ASTM International, West Conshohocken, PA. DOI: 10.1520/C0192_C0192M-25A.

ASTM International (2025). Standard test method for measuring the damage resistance of a fiber-reinforced polymer matrix composite to a drop-weight impact event (ASTM D7136/D7136M-25), ASTM International, West Conshohocken, PA. DOI: 10.1520/D7136_D7136M-25.

ASTM International (2021). Standard test method for slump flow of self-consolidating concrete (ASTM C1611/C1611M-21), ASTM International, West Conshohocken, PA. DOI: 10.1520/C1611_C1611M-21.

Al-Hadithi, A.I., Hilal, N.N., Al-Gburi, M. and Midher, A.H. (2023) "Structural behavior of reinforced lightweight self-compacting concrete beams using expanded polystyrene as coarse aggregate and containing polyethylene terephthalate fibers", *Structural Concrete*, 24(5), 5808–5826. https://doi.org/10.1002/suco.202200381

Alobaidi, Y.M., Hilal, N.N. and Faraj, R.H. (2021) "An experimental investigation on the nano-fly ash preparation and its effects on the performance of self-compacting concrete at normal and elevated temperatures", *Nanotechnology for Environmental Engineering*, 6(2), 1–13. https://doi.org/10.1007/s41204-020-00098-6

Al-Sebai, H., Al-Sadoon, Z.A., Altoubat, S. and Maalej, M. (2024) "Constitutive relations for modelling macro synthetic fiber reinforced concrete", *Civil Engineering Journal*, 10(6), 1806–1823. https://doi.org/10.28991/CEJ-2024-010-06-06

Asmaa, H.S. and Khashaa Mahmoud, M. (2022) "Optimum characteristics of plastic fibres for sustainable self-compacting concrete SCC", *European Journal of Environmental and Civil Engineering*, 27(9), 2967–2984. https://doi.org/10.1080/19648189.2022.2119605

Askar, K., Yaman, S.S., Al-Kamaki, S. and Hassan, A. (2023) "Utilizing polyethylene terephthalate PET in concrete", *Polymers*, 15(15), 1–32. https://doi.org/10.3390/polym15153320

Ayub, T., Khan, S.U. and Mahmood, W. (2022) "Mechanical properties of self-compacting rubberised concrete (SCRC) containing polyethylene terephthalate (PET) fibres", *Iranian Journal of Science and Technology, Transactions of Civil Engineering*, 46(2), 1073–1085. https://doi.org/10.1007/s40996-020-00568-6

Azarsa, P. and Gupta, R. (2020) "Freeze-thaw performance characterization and leachability of potassium-based geopolymer concrete", *Journal of Composites Science*, 4(2), 1–18. https://doi.org/10.3390/jcs4020045

Basser, H., Moradi Shaghaghi, T., Afshin, H., Saleh Ahari, R. and Mirrezaei, S.S. (2022) "An experimental investigation and response surface methodology-based modeling for predicting and optimizing the rheological and mechanical properties of self-compacting concrete containing steel fiber and PET", *Construction and Building Materials*, 315(2), 125370. https://doi.org/10.1016/j.conbuildmat.2021.125370

Deng, Y. and Li, Y. (2025) "Exploring the enhanced dispersibility of silane coupling agent–modified basalt fiber and its impact on concrete mechanical properties", *Journal of Materials in Civil Engineering*, 37(2), 04024324. https://doi.org/10.1061/JMCEE7.MTENG-18471

Flores Nicolás, A., Menchaca Campos, E.C., Flores Nicolás, M., Gonzalez Noriega, O.A., García Peréz, C.A. and Uruchurtu Chavarín, J. (2024) "Corrosion resistance of reinforcing steel in concrete using natural fibers treated with used engine oil", *Civil Engineering Journal*, 10(4), 1012–1027. https://doi.org/10.28991/CEJ-2024-010-04-02

Gholhaki, M., Aljenab, A. and Rezayfar, O. (2022) "Investigation and extraction of compressive strengths of concrete containing zeolite and bentonite, according to the dimensions and type of samples (cubic and cylindrical) at different temperatures", *Journal of Structural and Construction Engineering*, 9(8), 138–158. https://doi.org/10.22065/jsce.2022.303890.2566

Gupta, M., Raj, R. and Sahu, A.K. (2022) "Mechanical properties of high strength concrete incorporating chopped basalt fibers: experimental and analytical study", *Materials*

Research Express, 9(12), 125–305. https://doi.org/10.1088/2053-1591/aca644

Hemati, S.A., Derakhshan Nezhad, A.H. and Rezaifar, O. (2025) "Predicting compressive strength of heavyweight concrete using deep neural networks and Box–Behnken design", *Challenge Journal of Concrete Research Letters*, 16(4), 173–202. https://doi.org/10.20528/cjcrl.2025.04.002

Imran Khan, M., Umair, M., Shaker, K., Basit, A. and Kashif, M. (2020) "Impact of waste fibers on the mechanical performance of concrete composites", *Journal of The Textile Institute*, 111(11), 1632–1640. https://doi.org/10.1080/00405000.2020.1736423

Iqbal, M., Zhang, D., Khan, M.I., Zahid, M. and Jalal, F.E. (2023) "Effects of rebar size and volume fraction of glass fibers on tensile strength retention of GFRP rebars in alkaline environment via RSM and SHAP analyses", *Journal of Materials in Civil Engineering*, 35(9), 23–45. https://doi.org/10.1061/JMCEE7.MTENG-15589

Jaskowska-Lemańska, J., Kucharska, M., Matuszak, J., Nowak, P. and Łukaszczyk, W. (2022) "Selected properties of self-compacting concrete with recycled PET aggregate", *Materials*, 15(7), 25–66. https://doi.org/10.3390/ma15072566

Kareem, M.A., Ajadi, E.O., Fadipe, O.O., Ishola, K., Olawuyi, O.A., Ayanlere, S.A., Olatoyan, O.J., Adeosun, J.O., Adefajo, A.A., Oyewo, A.T., Olawale, S.O.A. and Lamidi, W.A. (2025) "Sustainability-driven application of waste steel and tyre rubber fibres as reinforcement in concrete: An optimization study using response surface methodology", *Next Materials*, 7(10), 30–45. https://doi.org/10.1016/j.nxmate.2024.100345

Khashaa, M., Ismail, A. and Marwa, H. (2019) "Production and optimization of eco-efficient self-compacting concrete SCC with limestone and PET", *Construction and Building Materials*, 197(10), 734–746. https://doi.org/10.1016/j.conbuildmat.2018.11.189

Li, Z., Yin, P., Liu, F., Pan, B. and Liu, Y. (2024) "Composite Design of a Phosphogypsum Whisker–Based Rejuvenator Based on the RSM and Evaluation of the Rejuvenating Effect", *Journal of Materials in Civil Engineering*, 37(1), 43–73. https://doi.org/10.1061/JMCEE7.MTENG-18699

Liang, Y., Zheng, S., Yang, Z. and Wang, X. (2024) "Optimization of mix proportions for hybrid fiber engineered cementitious composites based on Box-Behnken design response surface model", *Construction and Building Materials*, 421(2), 56–97. https://doi.org/10.1016/j.conbuildmat.2024.135697

Mirzaie Aliabadi, M., Derakhshan Nezhad, A.H., Shahidzadeh, M.S. and Dadpur, A. (2025a) "Date palm fibers to improve tensile strength in self-compacting concrete with silica fume", *Civil Engineering Infrastructures Journal*, 58(2), 333–349. https://doi.org/10.22059/ceij.2024.368987.1988

Mirzaie Aliabadi, M. Zadeh, M.S.S. and Derakhshan Nezhad, A.H. (2025b). "Analyzing and examining the impact of various fiber types on the mechanical and functional characteristics of UHPC", *Research in Engineering Structures and Materials*, 11(3), 1219–1244. https://doi.org/10.17515/resm2024.367me0725rs

Rashwan, M.A., Al Basiony, T.M., Mashaly, A.O. and Khalil, M.M. (2022) "Self-compacting concrete between workability performance and engineering properties using natural stone wastes", *Construction and Building Materials*, 319(3), 26–32. https://doi.org/10.1016/j.conbuildmat.2021.126132

Sunardi, S., Ariawan, D., Surojo, E., Prabowo, A.R., Ghanbari-Ghazijahani, T., Wibowo, C.H. and Akbar, H.I. (2024) "Tribological Performance of Polymer Composite Modified with Calcined Eggshell Particles Post High-Temperature Exposure", *Emerging Science Journal*, 8(4), 1280–1292. https://doi.org/10.28991/ESJ-2024-08-04-03

Widodo, S., Alfirahma, R., Prawiranegara, A., Amir, F. and Dewi, A. (2023) "Development of Eco-friendly Self-compacting Concrete Using Fly Ash and Waste Polyethylene Terephthalate Bottle Fiber ", *Civil Engineering Journal*, 9(2), 437–452. https://doi.org/10.28991/CEJ-2023-09-02-014

Xue, Z., Qi, P., Yan, Z., Pei, Q., Zhong, J. and Zhan, Q. (2023) "Mechanical Properties and Crack Resistance of Basalt Fiber Self-Compacting High Strength Concrete: An Experimental Study", *Materials*, 16(12), 43–74. https://doi.org/10.3390/ma16124374

Yang, X., Wang, Z., Wang, X., Wen, Y., Du, Y. and Ji, F. (2024) 'Study on Mechanical Properties of Nano-TiC- and Nano-SiO2-Modified Basalt

Fiber Concrete", *Buildings*, 14(7), 1–20. https://doi.org/10.3390/buildings14072120